Effect of Shear History on the Morphology of Immiscible Polymer Blends

Mario Minale, Paula Moldenaers,* and Jan Mewis

Department of Chemical Engineering, Katholieke Universiteit Leuven, de Croylaan 46, B 3001 Heverlee, Leuven, Belgium

Received November 26, 1996; Revised Manuscript Received June 20, 1997[⊗]

ABSTRACT: In this paper we study how the steady state morphology during shear of an incompatible blend can be affected by the initial conditions. By means of rheological experiments it is shown that below a critical shear rate multiple steady states can be obtained, the final morphology being then determined by the initial conditions of the blend. Above the critical shear rate the morphology is univocally determined by an equilibrium between break-up and coalescence. The critical shear rate is identified as the value at which the break-up limiting curve crosses the coalescence one. The applicability of different coalescence theories has been investigated by changing the viscosity ratio. The different coalescence theories can all describe the experimental results with a reasonable precision. The accuracy of the fully mobile interface theory seems to increase with decreasing viscosity ratio, whereas the opposite holds for the immobile interface theory. The partially mobile interface theory describes the various results equally well.

Introduction

Polymer blending has gained interest as a very suitable alternative for the synthesis of new monomers to generate materials with improved properties. In an incompatible blend the mechanical properties are not totally determined by those of the component polymers, they are also strongly affected by the morphology of the blend. This is in turn affected by the flow conditions during blending and subsequent processing. Hence it is of crucial importance not only to be able to probe *ex post facto* the morphology that results from blending two immiscible polymers but also to predict it.

The morphology of a blend has generally been assumed to be a unique function of the flow history and of the properties of the polymers used. As a consequence, the steady state morphology of a given blend has been considered to be a single valued function of the characteristics of the applied flow,[1,2] being the result of an equilibrium between a break-up and a coalescence process. Nevertheless, it has been pointed out in the literature that there might be flow conditions in which more than one steady state morphology could be obtained.[3] When multiple steady states are possible, the final morphology will depend on the prior state, i.e., on the initial conditions. Here the effect of the initial conditions on the steady state morphology of an incompatible polymer blend will be studied. As coalescence plays a major role in morphology development, the investigation will also provide an opportunity to evaluate coalescence models.

Materials and Methods

To study the relation between flow and morphology, it is indicated to start with a model blend the components of which are almost inelastic, so that the elastic characteristics of the blend can be attributed to interfacial contributions. A mixture of a polyisobutylene (PIB Parapol 1300 from Exxon) and a poly(dimethylsiloxane) (PDMS Rhodorsil 47V100000 from Rhône-Poulenc) has been chosen for this purpose. Their relevant physical characteristics are summarized in Table 1. The Newtonian viscosities of the pure polymers nearly match at 23 °C. As their activation energies differ considerably, the viscosity ratio of the blend can be altered by changing the temperature. The polymers are liquid at room temperature, thus avoiding degradation problems usually encountered with melts.

Table 1. Characteristics of the Pure Components[a]

	η_0 (Pa·s)	Ψ_1 (Pa·s^2)	ρ (kg m^{-3})	E_a (J mol^{-1})
PDMS (47V100000)	100	1.66	973[(1)]	1.393×10^4
PIB (1300)	92.7	0.09	894[(2)]	7.2×10^4

[a] All the data are referred to 23 °C with the exception of (1) which is at 25 °C and (2) which is at 20 °C.

As interfacial tension the value of 2.8×10^{-3} N·m^{-1} measured by Sigillo et al.[4] has been used. It was obtained on a blend very similar to the present one, the only difference being the grade of PDMS (PDMS Rhodorsil 47V200000 instead of the 47V100000), which has a higher molecular weight than the one investigated here. When the molecular weight of a polymer exceeds 3000, its surface tension becomes constant.[5] It is assumed that the interfacial tension behaves in the same way. Since the molecular weight of the PDMS under investigation exceeds this critical value, it seems acceptable to use the value of the interfacial tension of a blend with an higher molecular weight component. This assumption has been verified by measuring the interfacial tension with a rheo-optical technique developed in this laboratory.[6] It resulted in a value of $\sim 3 \times 10^{-3}$ N·m^{-1}, which is in excellent agreement with the value of reported by Sigillo et al. for the system with higher molecular weight component. This value is of the same order of magnitude as that of the industrially used mixtures of polymer melts.

The blends have been prepared according to a fixed procedure that has been used previously by Takahashi et al.[1] and Vinckier et al.[2] and has been proven to be adequate. Firstly, suitable amounts of the two components are mixed with a spatula for ca. 10 min until a homogeneous, white creamy appearance is obtained. The sample is then put overnight in a vacuum oven at room temperature to remove the entrapped air bubbles. The samples are then preconditioned, before each measurement, by shearing until a steady state morphology is attained. The amount of straining required to reach a steady state morphology for our blends has been determined in preliminary tests. Stress transients after a sudden increase in shear rate have been used for this purpose as they have been shown to be very sensitive to the initial morphology.[1,2] It was found that the stress profiles do not depend on the applied amount of prestrain anymore after a strain of the order

* To whom correspondence should be addressed.

[⊗] Abstract published in *Advance ACS Abstracts,* August 15, 1997.

S0024-9297(96)01733-0 CCC: $14.00

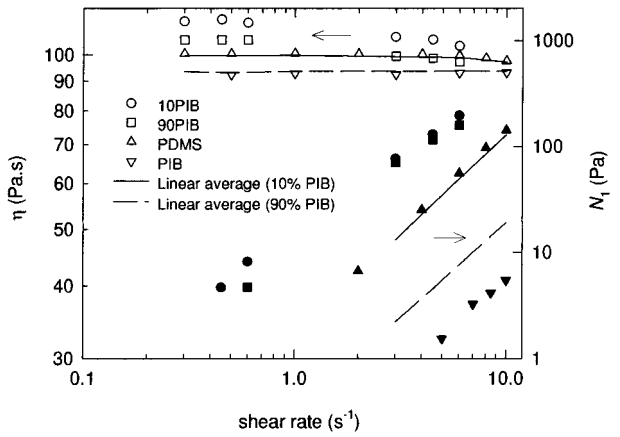

Figure 1. Steady state results at 23 °C for the 10PIB (p = 0.93) and 90PIB (p = 1.08) blends and for the pure components. The lines are the result of applying a linear mixing rule of the components properties.

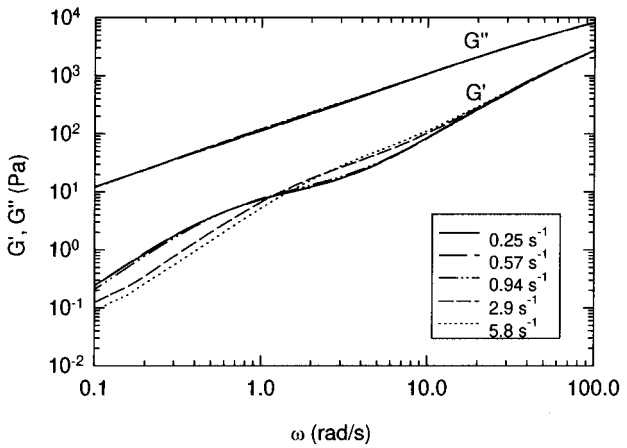

Figure 2. Dynamic moduli of the 10PIB blend at 23 °C after shearing at various shear rates. The experiments have been performed at increasing preshear rates.

of 2000, and this has been the minimum value used subsequently for preconditioning. The consequences of using this procedure will be discussed below. Systems with weight compositions of 10% PIB−90% PDMS (10PIB) and 90% PIB−10% PDMS (90PIB) have been selected for the experiments.

A strain-controlled rheometer (Rheometrics Mechanical Spectrometer RMS 800) has been used for the steady state measurements. It is equipped with a cone and plate geometry (diameter, 0.025 m and cone angle, 0.1 rad). This rather large angle minimizes the effect of a misalignment of the tool but narrows the range of the accessible shear rates as shear fracture appears at shear rates of approximately of 8−10 s^{-1}. The temperature has been controlled by means of a fluid bath, the test temperature being 23 ± 0.5 °C.

Dynamic experiments after stopping the flow have been performed on a stress-controlled rheometer (Rheometrics DSR). Also in this case a cone and plate geometry has been chosen (diameter, 0.025 m and cone angle, 0.1 rad) with test temperatures controlled by means of a Peltier element, ranging from 17 ± 0.1 to 28 ± 0.1 °C. A linearity check showed the behavior of the blend to be linear up to a strain amplitude of 10% for all the frequencies used. This implies that at these amplitudes the oscillatory motion does not induce real changes in the morphology but only perturbs it. It has also been verified that no bias from structural changes is present in the oscillatory experiments after stopping the flow. Indeed, coalescence after cessation of flow takes place on a time scale much longer than the duration of the experiments. On the other hand, the droplets of the blend recover their spherical shape very quickly; actually, this process is completed even before the first measurement point is recorded. Hence the dynamic experiments after cessation of flow probe the recoiled morphology of the blend, i.e., with spherical droplets as generated by the previous flow.

Steady State Results

In Figure 1 the steady state viscosities (η) and first normal stress differences (N_1) are presented as function of the shear rate, for the pure components as well as for the 10PIB blend (viscosity ratio p = 0.93 at T = 23 °C) and the 90PIB blend (viscosity ratio p = 1.08 at T = 23 °C). The pure components show a constant shear viscosity and a very small first normal stress difference proportional to the square of the shear rate (second-order behavior). Because of the limited elasticity of the pure components, all the elastic characteristics of the blend can be attributed to the interface.

The blends show a plateau viscosity at low shear rates. Its value exceeds the one obtained from a linear mixing rule of those of the pure components. Furthermore, shear thinning sets in around 1 s^{-1}. The first normal stress difference of both blends largely exceeds that of the components and tends to have a linear dependence on the shear rate, as suggested by Onuki[7] as well as by Doi and Ohta.[8] The Doi−Ohta theory can be applied in this relatively low concentration regime as long as the morphology of the blends is controlled by shear rate, i.e., as long as the blend does not possess an intrinsic length scale or equivalently an intrinsic relaxation time.

Dynamic Experiments after Cessation of Flow

For viscoelastic blends such as our model systems, linear dynamic measurements after cessation of flow have been proven to be a very sensitive tool to determine either the interfacial tension[9−11] or the average droplet diameter.[2] In this paper the linear dynamic moduli are used to study the evolution of the steady state droplet size of the blends as a function of shear rate, initial conditions, and viscosity ratio. In Figure 2 the dynamic moduli, G' and G'', are shown for the 10PIB blend at 23 °C (p = 0.93) with the steady state preshear rate as parameter. The experiments have been performed while increasing the preshear rates. The curves obtained after shear rates of 0.25, 0.57, and 0.94 s^{-1} almost coincide.

Once the storage moduli G' are available, it is possible to use an emulsion model (Palierne[12]) to estimate the volumetric mean radius of the blend. In this model the hydrodynamic interactions between the droplets are taken into account, to a certain extent. It can, therefore, also be applied to such nondilute blends as the ones under investigation. In the present case a simplified version of the model has been used since the interfacial tension tensor is considered to be isotropic; i.e., the interfacial tension is assumed not to depend on the local shear or on the deformation of the interface. This has been shown to lead to satisfactory results in the absence of interfacial agents,[9,13] which is the case for the model blends used in this study.

Although the entire distribution function of the droplet radii can be incorporated in the Palierne model, only their volumetric mean will be used here, as suggested by Graebling et al.[9,13] These authors pointed out that this is acceptable provided the polydispersity index of the blend does not exceed a value of about 2. The blends studied by Vinckier et al.[2] satisfied this requirement. As they only differ from those under investigation by the grade of PDMS, it seems reasonable to assume this approximation to be also applicable in

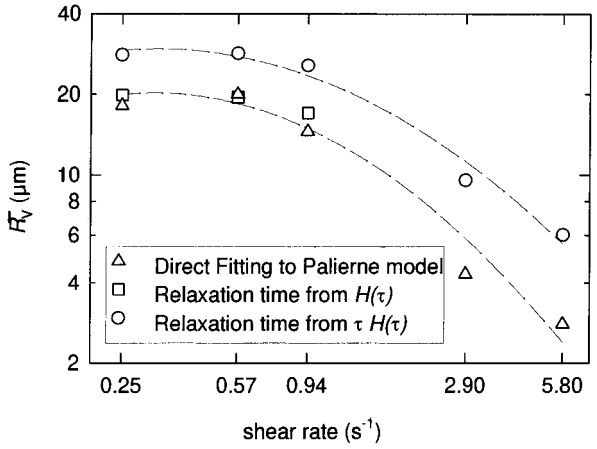

Figure 3. Volumetric average radius $\bar{R}_V$ as a function of the preshear rate, calculated with three methods (see text) from the spectra of Figure 2. The experiments have been performed while the preshear rate was increased. The lines are drawn to guide the eye.

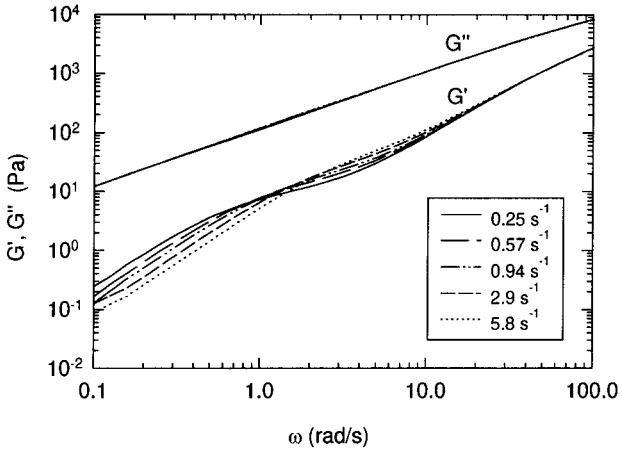

Figure 4. Dynamic moduli of the 10PIB blend at 23 °C for different shear rates. The experiments have been performed with decreasing preshear rates.

the present case. With these simplifications the Palierne model predicts

$$G' = \mathrm{Re}\left(G_m^* \frac{D + 3\phi E}{D - 2\phi E}\right) \quad (1)$$

with

$$D = (2G_d^* + 3G_m^*)(19G_d^* + 16G_m^*) + \frac{40\alpha}{\bar{R}_V}(G_d^* + G_m^*) \quad (2)$$

$$E = (G_d^* - G_m^*)(19G_d^* + 16G_m^*) + \frac{4\alpha}{\bar{R}_V}(5G_d^* + 2G_m^*) \quad (3)$$

where the subscripts m and d refer to the matrix and the dispersed phase, respectively, Re(x) is the real part of x, G^* the complex modulus, α the interfacial tension, and $\bar{R}_V$ is the unknown volumetric mean radius. The volumetric concentration of the dispersed phase (ϕ) coincides in our case with the weight concentration, the densities of the two components of the blend being almost the same (see Table 1).

To calculate the droplet size, different procedures can be applied. The first procedure consists of a least squares fit of the theoretical predictions of $G'(\omega)$ to the experimental results, using $\bar{R}_V$ as fitting parameter. In the other procedures it is necessary to determine first the relaxation time of the blend. The following approximate equation can be derived from the Palierne model:[9]

$$\tau = \frac{\eta_m \bar{R}_V}{4\alpha} \frac{(19p + 16)(2p + 3 - 2\phi(p + 1))}{10(p + 1) - 2\phi(5p + 2)} \quad (4)$$

where τ is the relaxation time and p, as already said, is the viscosity ratio of the blend. The characteristic time for droplet relaxation can be calculated either directly from the relaxation time spectrum, $H(\tau)$, of the blend or from its first moment $\tau H(\tau)$, as suggested by Gramespacher and Meissner.[11] The use of the first moment amplifies the contribution of the slower processes and therefore that of the interfacial relaxation.

Figure 3 shows the droplet mean radii as calculated from the dynamic spectra of Figure 2 with all three procedures, whenever possible. For the high shear rates the procedure using $H(\tau)$ may fail to isolate the relaxation of the interface because it is not amplified enough. In agreement with the observations of ref 2, the first and second procedures give, within experimental error, the same results whereas the third one leads to droplet radii which are a factor 2 larger. It is logical that the third procedure produces larger values than the second one as a higher order moment of the spectrum is used. Nevertheless, the functionality of the radius versus shear rate is the same with all three procedures. The morphology seems to remain constant until a shear rate of 0.7−0.8 s^{-1}; from thereon a refinement occurs.

In ref 2 it was shown that subtracting the average of the relaxation spectra of the pure components from $H(\tau)$ provides the most accurate value for the radii. For the present blends the use of $H(\tau)$ is adequate since the relaxation of the components is much faster than that of the interface. As $H(\tau)$ gives the same results as the direct fitting of $G'(\omega)$, only the results obtained with the latter method will be presented in the remainder.

To investigate the effect of changing the initial conditions, the dynamic moduli were also determined after cessation of flow while the preshear rate was decreased (Figure 4), rather than increased. A comparison between Figures 2 and 4 immediately shows that the spectra for a given shear rate do not always coincide. In fact, while in Figure 2 the spectra obtained after shear rates of 0.25, 0.57, and 0.94 s^{-1} almost coincide, they are well distinguishable in Figure 4. The volumetric mean radii for the sequence of decreasing shear rates are compared in Figure 5 with those obtained while increasing the shear rate (Figure 3). Only at the highest shear rates do the two sequences produce identical values for the average droplet radii; at lower shear rates the curves describe a hysteresis loop. The effect of concentration on the evolution of the droplet size with shear rate will be reported elsewhere.[14]

It is worthwhile to stress the importance of the observed hysteresis. The steady state morphology of a blend, seen as the equilibrium between a break-up and a coalescence process, is known to be a function of the characteristics of the material itself as well as of the applied flow. The shear rate dependency has generally been described by a single valued function. In contrast to this, the present experiments demonstrate that a unique morphology is in practice obtained only when the shear rate exceeds a certain critical value. At lower shear rates the morphology of the blend is affected by the initial conditions. To be sure that the morphologies that have been determined are steady state

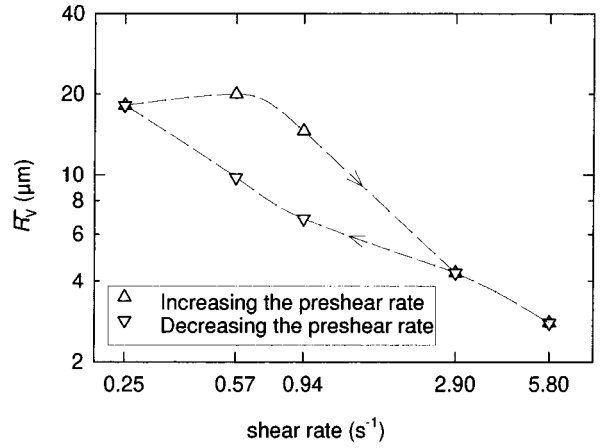

Figure 5. Comparison of steady state droplet radii obtained from experiments performed at increasing shear rates (Figure 2) and at decreasing shear rates (Figure 4). The lines are drawn to guide the eye. ($T = 23$ °C, $p = 0.93$.)

morphologies, or at least pseudo steady state ones, some of the experiments have been repeated with preshearing for up to 15 000−20 000 strain units, resulting in identical values for the radii as in earlier experiments. This does not completely exclude the possibility that a change in morphology on a much longer time scale could take place, but this seems to be almost irrelevant for all practical purposes.

Discussion

Morphological Hysteresis. In order to explain the difference between the experiments performed at increasing or decreasing shear rates (Figure 5), it is necessary to recall that the break-up and coalescence processes can occur only under certain conditions. Once the shear rate is fixed, the flow can only break droplets the radii of which are larger than a critical value and two droplets can only coalesce, at least with some reasonable probability, if their average radius is smaller than a critical one. A semiempirical limiting curve for break-up was derived by de Bruijn[15] from the experimental results of Grace[16] for isolated droplets:

$$\log\left(\frac{\eta_m \dot{\gamma} R}{\alpha}\right) = -0.506 - 0.0994 \log(p) + 0.124 \log^2(p) - \frac{0.115}{\log(p) - \log(p_{cr})} \quad (5)$$

where $\log(x)$ is the decimal logarithm of x and $p_{cr} = 4.08$ is the viscosity ratio above which break-up is not possible anymore in shear flow.

For the coalescence limit several theories have been suggested. They differ in the way in which the interface of the colliding droplets is treated. Assuming that the interface becomes flat in the collision area once it deforms, which is realistic for rather slow flows, the mobility of the interface will determine the boundary conditions for the squeezing flow of the matrix fluid between the approaching droplets. Three different theories can then be applied: the fully mobile interface (FMI[17]), the partially mobile interface (PMI[18]), and the immobile interface theory (IMI[19]).

In order to obtain the critical radius for coalescence, some approximations must be made.[3] The coalescence probability is defined as the product of the collision probability (P_{coll}) and the drainage probability (P_{drain}). These probabilities can be expressed as the negative exponential of the ratio of the time required for the phenomenon to take place to the available time: $\exp(-t_{req}/t_{avail})$. P_{coll} gives the probability that a collision between two droplets of mean radius R takes place during the available process time. This probability has been set to 1 because only steady state morphologies, or at least pseudo steady state ones, are involved and therefore the process time can in principle be considered to be infinitely long. P_{drain} is the probability that the collision leads to coalescence, i.e., the probability that the film of the matrix fluid located between the approaching droplets is drained within the duration of the collision. In this case t_{req} is the drainage time t_{drain}, while t_{avail} is the interaction time t_{int}. The coalescence theories give different expressions for the drainage time, whereas the interaction time, i.e., the duration of the collision, is always set as $1/\dot{\gamma}$. A binary approximation is done at this point: $P = 1$ if $t_{avail} \geq t_{req}$, and $P = 0$ if $t_{avail} < t_{req}$. This approximation, even if very crude, allows one to estimate the critical radius above which coalescence is unlikely to take place. With this approximation it is implicitly assumed that when the coalescence kinetics are slower than a certain critical value they are considered to be zero. Consequently, only pseudo steady states can be predicted, but as mentioned above, this seems to be relevant for all practical purposes. Finally, equating t_{drain} to $1/\dot{\gamma}$ for the different theories, the following limiting curves are obtained:[3]

FMI:
$$R \ln\left(\frac{R}{h_{cr}}\right) = \frac{2}{3}\frac{\alpha}{\eta_m \dot{\gamma}} \quad (6)$$

PMI:
$$R = \left(\frac{4}{\sqrt{3}}\frac{h_{cr}}{p}\right)^{2/5}\left(\frac{\alpha}{\eta_m \dot{\gamma}}\right)^{3/5} \quad (7)$$

IMI:
$$R = \left(\frac{32}{9}\right)^{1/4}\left(\frac{h_{cr}\alpha}{\eta_m \dot{\gamma}}\right)^{1/2} \quad (8)$$

where h_{cr} is the critical thickness of the fluid layer between the droplets below which the coalescence occurs and $\ln(x)$ is the natural logarithm of x. In the original paper by MacKay and Mason[19] the drainage time refers to a droplet of radius R coalescing on a flat layer. When dealing with two droplets of radius R, the drainage time must be corrected by a factor 4, even if this is not really crucial when only an estimation of it is required, this justifies the discrepancy between eq 8 and the corresponding one reported in ref 3. In order to deduce a critical value for R from the coalescence models, h_{cr} needs to be known. It is very difficult to determine this parameter experimentally. A theoretical prediction of h_{cr} is given by Chesters[20] as

$$h_{cr} \approx \left(\frac{AR}{8\pi\alpha}\right)^{1/3} \quad (9)$$

where A is the Hamaker constant, which is unknown for our pure components. Using eq 9 our ignorance is only displaced from h_{cr} to A. Furthermore, it is worthwhile to remember that all these theories have been deduced for an isolated pair of droplets, while the incompatible blend investigated here is rather concentrated; therefore, in this paper h_{cr} has been considered as an adjustable parameter.

The limiting curves, given by eqs 5−8, together with the experimental data of Figure 5 are reported in Figure 6. The factor h_{cr} has been adjusted by imposing the coalescence curves to pass through point 1 = 1′. A

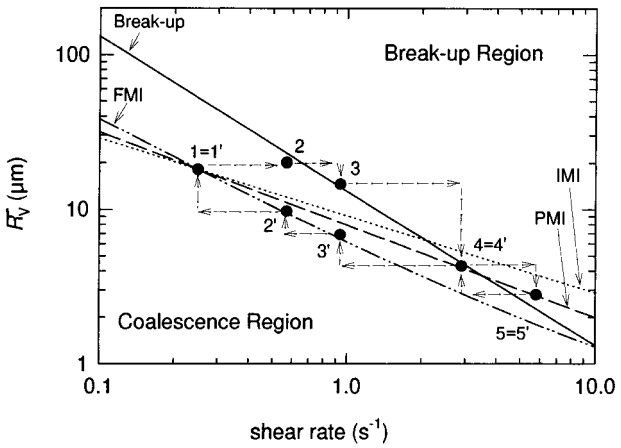

Figure 6. Data at 23 °C ($p = 0.93$) from Figure 5 together with the theoretical limiting curves for break-up and coalescence. Three different theories for the coalescence are considered. The arrows indicate the order in which the experiments have been performed.

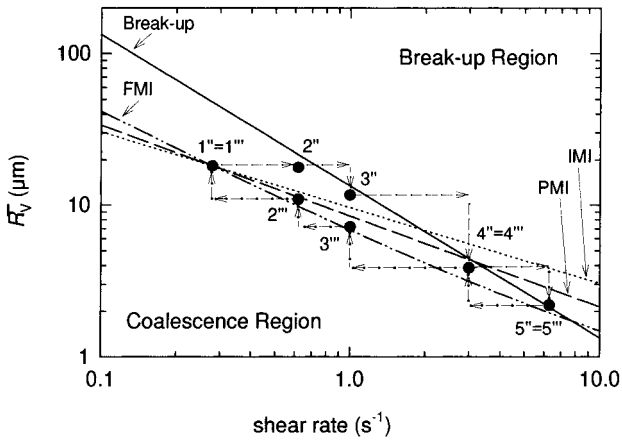

Figure 7. $\bar{R}_V$ obtained at 28 °C for the 10PIB blend ($p = 0.625$) while the preshear rate was increased and decreased. The theoretical limiting curves are also shown.

critical shear rate is then immediately identified as the point at which the break-up limit curve crosses the coalescence one. Since the coalescence limit is a weaker function of $\dot{\gamma}$ than the break-up one, see eqs 5−8, there is a zone, below the crossover point, where neither coalescence nor break-up can occur. As a result, no equilibrium between the two processes can be reached and hence more than one morphology is possible at a given shear rate.

With the previous argument the experimental results can now be explained. Points $4 = 4'$ and $5 = 5'$ can be considered as equilibrium points and hence they are not affected by the initial conditions of the blend. The other points, however, do not result from an equilibrium between break-up and coalescence but are determined by only one of the two processes. In the sequence $3'-2'-1'$, coalescence is the only phenomenon that can occur; the points lie indeed on the limiting curve for this mechanism, while break-up will determine the morphology in sequence 1−2−3, at least from the point where the limiting curve for break-up is crossed when the shear rate is increased. Actually, moving from point 1 to point 2, the "dead" zone, the region where neither coalescence nor break-up can take place, is entered and hence the radius remains constant. Between points 2 and 3 the break-up limit is crossed and the morphology refines until the break-up limit is again reached (point 3).

The fact that at $\dot{\gamma} = 0.25$ s^{-1} there is no difference between point 1 and point $1'$ leads to the conclusion that point 1 has been reached by the coalescence process only. Therefore the initial morphology of the blend after the sample loading must have been characterized by a mean radius smaller than 18 μm. The value of h_{cr} has indeed been estimated by imposing the coalescence curves to pass through point $1 = 1'$. The resulting values for h_{cr} are 3.0×10^{-7} m in the FMI case, 4.8×10^{-7} m in the PMI case, and 2.2×10^{-6} for the IMI theory. They are 1−3 orders of magnitude larger than the typical value suggested by Chesters.[20] This can possibly be explained by the unavoidable presence of dust particles in the blend that contaminate the interface or by the fact that we are dealing with a concentrated blend for which it is not surprising that the coalescence phenomenon is more effective than predicted by Chesters for an isolated pair of droplets. In fact, for a concentrated blend P_{drain} can be greater than that for an isolated pair of drops, essentially because t_{avail} can be longer due to the interaction between droplets. Since t_{avail} has been fixed to be $1/\dot{\gamma}$ the only way to take into account this increase of P_{drain} is through t_{drain}, i.e., through the unknown h_{cr}. Consequently, in a concentrated blend h_{cr} looses its physical meaning, carrying with it all the uncertainties and the approximations of the model and therefore it can only be considered as an adjustable parameter. The effect of concentration on h_{cr} has been studied separately.[14] Grizzuti et al.[21] have observed in their blend, via microscopy, a similar hysteresis phenomenon, obtaining an estimate of h_{cr} that is of the same order of magnitude as the one calculated here.

Evaluation of Coalescence Theories. Up to now no comments have been made about the applicability of the different coalescence theories, and indeed, Figure 6 shows that, even if the PMI seems to work slightly better than the other ones, all three theories can qualitatively describe the experimental results. To be able to draw some conclusions on this subject, it is useful to study the hysteresis phenomenon as a function of temperature. With the 10PIB blend the viscosity ratio is changed by varying the temperature, the activation energy of PIB being much larger than that of PDMS. Hence, changing the temperature offers the opportunity to perform a similar series of experiments on blends with different viscosity ratios. At the same time the interfacial tension is also altered, in ref 22 the temperature coefficient $d\alpha/dT$ is reported to be -0.03×10^{-3} $N \cdot m^{-1} \cdot K^{-1}$.

The experimental data obtained at 28 °C ($p = 0.625$) are presented in Figure 7 together with the limiting curves. The coalescence limit is now shifted toward higher radii for all three theories; on the contrary the break-up limit remains almost the same as for 23 °C. The hysteresis occurs again for shear rates below 3 s^{-1}. The values of h_{cr} have been estimated as before, producing the values of 4.0×10^{-7} m in the FMI case, 3.6×10^{-7} m for the PMI theory, and 2.4×10^{-6} m for the IMI one. The interfacial tension at 28 °C was found to be 2.65×10^{-3} $N \cdot m^{-1}$.

The results obtained at 17 °C ($p = 1.51$) are reported in Figure 8, the values of h_{cr} are now 2.9×10^{-7} m in the FMI case, 7.9×10^{-7} m in the PMI one, and 2.3×10^{-6} m for the IMI theory, the interfacial tension being 2.98×10^{-3} N m^{-1}. The hysteresis now appears also at $\dot{\gamma} \approx 2.5$ s^{-1} (points 4^{iv} and 4^{v}). The extension of the hysteresis region can be explained qualitatively with all

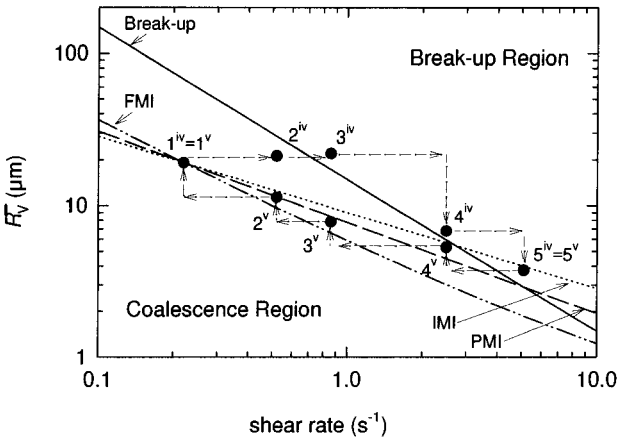

Figure 8. $\bar{R}_V$ obtained at 17 °C for the 10PIB blend ($p = 1.51$) while the preshear rate was increased and decreased. The theoretical limiting curves are also shown.

three theories. At $T = 17$ °C the break-up limit is shifted toward higher radii whereas the coalescence curves move toward smaller radii for all three theories. Consequently, the resulting critical shear rate moves to higher shear rates, thus enlarging the hysteresis region.

From a comparison of Figures 6−8 it is clear that the PMI theory can describe the results with the same accuracy at all three temperatures. On the contrary the agreement between the experimental data and the theoretical prediction obtained with the IMI theory improves as the viscosity ratio increases, whereas the agreement between the FMI prediction and the experimental results improves as the viscosity ratio decreases. This is in agreement with the hypotheses at the basis of these theories. In fact a fully mobile interface can be realized only with inviscid droplets, an immobile interface requires either a compatibilizer or a droplet phase with a viscosity much higher than that of the continuous phase. A partially mobile interface will be the result when the previous conditions are not met, i.e., for a viscosity ratio of the order 1.

Conclusions

The effect of the initial conditions on the steady state morphology of an incompatible model blend has been investigated. It has been shown experimentally that there is a critical shear rate above which a unique morphology is attained regardless of the initial conditions. This morphology results from an equilibrium between a break-up and a coalescence process. Below this critical shear rate, multiple steady states, or pseudo steady states, are possible and therefore the final morphology will not only depend on the characteristics of the applied flow but also on the initial conditions of the blend. The critical shear rate has been identified as the point at which the limiting curve for break-up crosses that for coalescence.

In the literature, several coalescence theories have been proposed. In order to identify the most appropriate the experiments have been repeated at different temperatures, resulting in blends with different viscosity ratios. It has been shown that the accuracy of the fully mobile interface theory increases as the viscosity ratio decreases whereas that of the immobile interface theory decreases. The partially mobile interface theory describes the experimental results with the same accuracy at all the three viscosity ratios investigated.

Acknowledgment. We would like to acknowledge DSM Research for having partially funded this research. Partial financial support for this project has been also provided by Onderzoeksfonds K. U. Leuven and FKFO. We also acknowledge Rhône-Poulenc for supplying the PDMS. The assistance of Peter van Puyvelde in performing the interfacial tension measurements is kindly acknowledged. The authors are indebted to Prof. N. Grizzuti for useful discussions.

References and Notes

(1) Takahashi, Y.; Kurashima, N.; Noda, I.; Doi, M. *J. Rheol.* **1994**, *38*, 699−712.
(2) Vinckier, I.; Moldenaers, P.; Mewis, J. *J. Rheol.* **1996**, *40*, 613−631.
(3) Janssen, J. Ph.D. Thesis, Eindhoven University of Technology, 1993.
(4) Sigillo, I.; di Santo, L.; Guido, S.; Grizzuti, N. *Polym. Eng. Sci.*, in press.
(5) Kobayashi, H.; Owens, M. J. *Trends Polym. Sci.* **1995**, *3*, 330−335.
(6) Van Puyvelde, P.; Moldenaers, P.; Mewis, J. Submitted for publication to *J. Colloid Interface Sci.*
(7) Onuki, A. *Phys. Rev. A* **1986**, *34*, 3528−3530.
(8) Doi, M.; Ohta, T. *J. Chem. Phys.* **1991**, *95*, 1242−1248.
(9) Graebling, D.; Muller, R.; Palierne, J. F. *Macromolecules* **1993**, *26*, 320−329.
(10) Graebling, D.; Benkira, A.; Gallot, Y.; Muller, R. *Eur. Polym. J.* **1994**, *30*, 301−308.
(11) Gramespacher, H.; Meissner, J. *J. Rheol.* **1992**, *36*, 1127−1141.
(12) Palierne, J. F. *Rheol. Acta* **1990**, *29*, 204−214.
(13) Graebling, D.; Muller, R.; Palierne, J. F. *J. Phys. IV* **1993**, *3*, 1525−1534.
(14) Minale, M.; Moldenaers, P.; Mewis, J. Submitted for publication to *AIChE J.*
(15) de Bruijn, R. A. Ph.D. Thesis, Eindhoven University of Technology, 1989.
(16) Grace, H. P. *Chem. Eng. Commun.* **1982**, *14*, 225−227.
(17) Chesters, A. K. *Int. J. Multiphase Flow* **1975**, *2*, 191−212.
(18) Chesters, A. K. *Euromech 234 − Int. Conf. Turbulent Two Phase Flow Systems*, Toulouse France **1988**.
(19) MacKay, G. D. M.; Mason, S. G. *Can. J. Chem. Eng.* **1963**, *41*, 203−212.
(20) Chesters, A. K. *Trans. IChemE* **1991**, *69A*, 259−270.
(21) Grizzuti, N.; Bifulco, O. Submitted for publication to *Rheol. Acta*.
(22) Koberstein, J. T. In *Concise Encyclopedia of Polymer Science and Engineering*; Kroschwitz, I. J., Ed.; Wiley: New York, 1990; pp 486−489.

MA9617330